Hybrid *s*-wave superconductivity in CrB$_2$

Sananda Biswas [1,*] Andreas Kreisel [2,3,†] Adrian Valadkhani,[1] Matteo Dürrnagel [4,5] Tilman Schwemmer [4]
Ronny Thomale,[4] Roser Valentí [1] and Igor I. Mazin[6,7]

^{1}*Institut für Theoretische Physik, Goethe-Universität Frankfurt, 60438 Frankfurt am Main, Germany*
^{2}*Institut für Theoretische Physik, Universität Leipzig, Brüderstraße 16, 04103 Leipzig, Germany*
^{3}*Niels Bohr Institute, University of Copenhagen, 2100 Copenhagen, Denmark*
^{4}*Julius-Maximilians-Universität Würzburg, 97070 Würzburg, Germany*
^{5}*Institute for Theoretical Physics, ETH Zürich, 8093 Zürich, Switzerland*
^{6}*Department of Physics and Astronomy, George Mason University, Fairfax, Virginia 22030, USA*
^{7}*Quantum Science and Engineering Center, George Mason University, Fairfax, Virginia 22030, USA*

In a metal with multiple Fermi pockets, the formation of *s*-wave superconductivity can be conventional due to electron-phonon coupling or unconventional due to spin fluctuations. We analyze the hexagonal diboride CrB$_2$, which is an itinerant antiferromagnet at ambient conditions and turns superconducting upon increasing pressure. While the high-pressure behavior of T_c suggests conventional *s*-wave pairing, we find that spin fluctuations promoting unconventional *s*-wave pairing become important in the vicinity of the antiferromagnetic dome. As the symmetry class of the *s*-wave state is independent of its underlying mechanism, we argue that CrB$_2$ is a realization of a *hybrid s*-wave superconductor where unconventional and conventional *s*-wave mechanisms team up to form a joint superconducting dome.

Introduction. Even though the phenomenological description of a superconducting state finds its common ground in the notion of a phase-coherent superposition of Cooper pairs and the mean-field description derived thereof [1], the possible microscopic formation mechanism is highly diverse. In a so-called conventional superconductor (CS), electron-phonon coupling generates an effective attractive electron-electron interaction [2–4]. Not only do phonons promote zero-angular-momentum Cooper pairs, i.e., an *s*-wave type pairing function, but the electron-phonon interaction also tends to be relatively momentum independent, a few exceptions not withstanding, and gives rise to a reasonably uniform gap, $\Delta_{CS}(\mathbf{k}) \sim$ const, throughout the Brillouin zone.

For unconventional superconductivity (UCS), which has most prominently surfaced in the context of the high-T_c cuprates, the microscopic footing of pairing appears both more diverse and less understood. From the viewpoint of spin fluctuations [5], electron pairing can originate from repulsive electron-electron interactions [6,7]. However, this implies that the gap function is sign changing in the Brillouin zone, leading to the condition $(\langle\Delta_{UCS}(\mathbf{k})\rangle_{BZ}^2 \ll \langle\Delta_{UCS}^2(\mathbf{k})\rangle_{BZ})$. For a single-pocket Fermi surface, this naturally suggests the presence of nodes and thus a principal unconventional superconducting gap that is qualitatively different from the conventional one. For multiple Fermi pockets, however, nodes are avoidable for unconventional pairing by allowing sign changes of Δ between the pockets. This is at the heart of the nature of superconducting pairing in iron pnictide superconductors [8,9],

where the compensated metal parent state forms superconducting pairing of opposite sign for hole and electron pockets, respectively. For each individual pocket, the gap may appear rather uniform, even though typically not as uniform as for a conventional superconducting state. Note that from the viewpoint of symmetry, such an unconventional superconducting gap cannot be distinguished from a conventional *s* wave: in both cases, the zero-momentum Cooper pair is described by the irreducible point-group representation with trivial characters. Yet, even though the *angular* dependence of the superconducting gap as a function of the wave vector is the same, the *radial* part shifts away from approximately constant in the conventional superconductor, referred to as s_{++}, to exhibit strong k dependence in the unconventional case, which is referred to as s_{+-}.

Since an *s*-wave superconductor can exist both as a conventional s_{++} and as an unconventional s_{+-}, in principle, a *hybrid s-wave superconductor* can be imagined, where unconventional and conventional pairing mechanisms team up to yield one continuous *s*-wave superconducting region spanning both CS and UCS domains. This intriguing possibility, however, requires a hypothetical material where spin fluctuations and phonons have a possibility to cooperate at least to some extent. More specifically, the latter have to peak at small wave vector, while the former (as long as we are not considering triplet pairing) necessarily have to have a maximum at a particular wave vector matching the Fermi surface geometry.

While iron pnictide superconductors seem to be a promising host for a hybrid superconducting state, the conventional and unconventional pairing are too imbalanced because of good Fermi-surface nesting enhancing the spin-fluctuation (SF) mechanism, as compared to weak electron-phonon
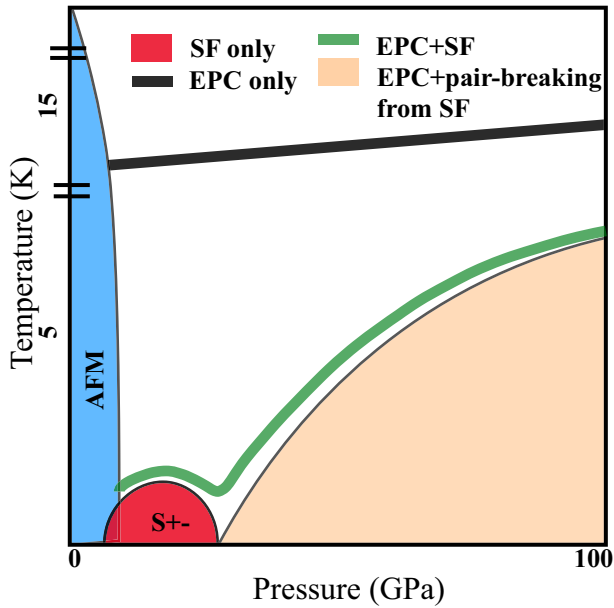
*biswas@itp.uni-frankfurt.de
†kreisel@nbi.ku.dk

FIG. 1. Proposed schematic temperature-pressure phase diagram for a hybrid *s*-wave superconductor. Spin fluctuation limit: Antiferromagnetic region with maximum T_{AFM} at ambient pressure (blue region), dropping rapidly with pressure and followed by (possibly overlapping with) a smaller unconventional superconducting dome near the quantum critical point (red region). Electron-phonon limit: T_c is only weakly dependent on pressure and dominates the high-pressure part of the phase diagram (light-orange region). The hybrid *s* wave (green) appears in the crossover region between the two limits where the pair-breaking impact of spin fluctuations is vital for explaining the drop of T_c towards ambient pressure.

coupling (EPC) [10]. In addition, EPC does not satisfy the requirement to peak at small q (i.e., in the intraband channel) either. In fact, the competition between SF and EPC has been under scrutiny for quite a few superconducting materials [11–15], but no suitable candidate has been identified so far, exhibiting not only competition, but also collaboration between the two mechanisms in some range of parameters.

In this Letter, we propose CrB_2 as a potential hybrid *s*-wave superconductor, continuously tunable by pressure between the s_{+-} and s_{++} limits. Indeed, superconductivity has recently been discovered in CrB_2 under pressure, with a maximum T_c of 7 K [16]. Isostructural to the conventional superconductor MgB_2 [17,18], CrB_2 exhibits itinerant antiferromagnetism at ambient pressure. T_c is found to weakly increase with pressure at odds with the typical dome formation in unconventional superconductors. This is a strong indication that at least beyond a certain pressure regime, superconducting pairing in CrB_2 is dominated by the electron-phonon coupling. Due to the proximity to the antiferromagnetic order, however, the superconductivity in CrB_2 is likely to be of unconventional nature at lower pressure, since spin fluctuations are crucial near a magnetic quantum critical point. From our synoptic analysis of superconductivity, accounting for both electron-phonon coupling and spin fluctuations, we find that CrB_2 is a likely candidate for a hybrid *s*-wave superconductor, as summarized in Fig. 1. On the one hand, spin fluctuations promoting s_{+-} type are highly relevant due to significant nesting of the

CrB_2 Fermi surface (note that here the three-dimensional nesting is present due to the flat parts in the Fermi surface in the k_x-k_y plane with large density of states). On the other hand, our calculations yield rather strong electron-phonon coupling, with the main contribution coming from around the Brillouin-zone center, Γ, enabling a significant cooperative effect between the two mechanisms. The interplay of both pairing tendencies culminates in the schematic temperature-pressure phase diagram depicted in Fig. 1 (green line): The superconducting domain in the high-pressure limit is dominated by the electron-phonon mechanism, which, if let alone, would suggest a fairly constant T_c throughout the phase diagram (black line) with no indication for competitive orders. By contrast, only spin fluctuations related to the antiferromagnetic order at the ambient pressure would generate unconventional superconductivity within a small pressure range and a significantly lower T_c than T_{AFM} (red dome). Taken together, however, electron-phonon couplings and spin fluctuations suggest a crossover between the two limiting scenarios, where, starting from the center of the superconducting region, spin fluctuations act upon the *s*-wave superconductor as pair breakers close to the antiferromagnetic phase at lower pressure and the electron-phonon coupling determines the scale of saturating superconducting pairing for higher pressure.

Methods. First, we investigate the superconducting pairing from a pure electron-electron interaction perspective adapting the spin-fluctuation pairing mechanism expected to be present for the correlated Cr $3d$ orbitals. To this end, we set up the pairing interaction in the random-phase approximation (RPA) [19,20] and solve the linearized gap equation for a discretization of the three-dimensional Fermi surface [21–23], yielding the eigenvalues, λ_i, and the gap eigenfunctions, $g_i(\mathbf{k})$, proportional to the superconducting order parameter. Next, we examine the electron-phonon mechanism by calculating the pressure dependence of the phonon dispersion, electron-phonon linewidth, γ, and electron-phonon coupling constants, λ, using density functional perturbation theory as implemented in the QUANTUM ESPRESSO code [24].

Results. CrB_2 crystallizes in a $P6/mmm$ structure (space group 191) with $c/a > 1$ at ambient pressure. As a function of pressure the c parameter decreases more rapidly than a, and around 30 GPa the ratio c/a becomes less than 1 with no observed changes in the crystal structure [16]. While the Mg states in MgB_2 lie far away from the Fermi surface, the band structure of CrB_2 suggests significant contributions from Cr $3d$ orbitals near the Fermi surface at all pressures (see Fig. 2 for the 100 GPa case), along with contributions coming from B atoms [23]. This makes the properties of CrB_2 markedly different from the isostructural MgB_2 [25], as we will discuss below. Accounting for the spin-density-wave instability at low pressures [16,26], we tune the bare Coulomb interaction responsible for the spin fluctuations such that the RPA instability occurs roughly at $p_c = 16$ GPa and then calculate pairing eigenvalues λ_i as a function of pressure. Figure 3 reveals the two main results from this investigation: First, the eigenvalues λ_i and therefore also the pairing strength rapidly decrease as a function of pressure, making this pairing interaction practically irrelevant at large pressures. Second, the leading instability is clearly of sign-changing s_{+-} type over a large pressure range with one exception very close to
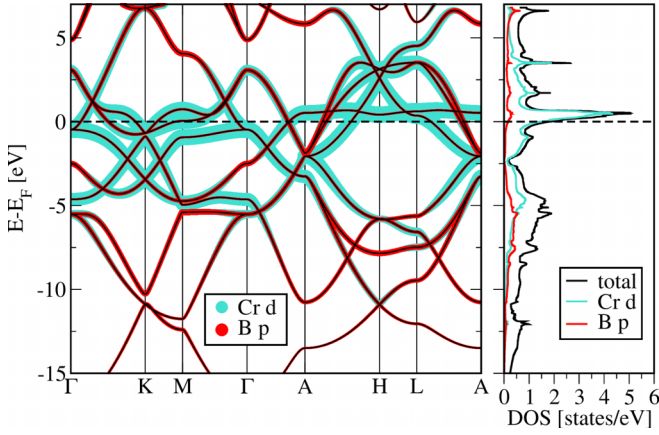
FIG. 2. Electronic band structure and density of states (DOS) at 100 GPa. Fat bands and DOS of Cr $3d$ states (cyan) and B $2p$ states (red) show that both states contribute to the formation of the Fermi surface.

p_c. The order parameter has one sign at a band forming a flat part at finite k_z close to the Brillouin zone boundary and opposite sign at the Fermi surface appearing around the Γ point (see Supplemental Material [23] for top views). Higher order s-wave solutions or solutions with higher angular momentum are subleading and their eigenvalues exhibit peaks from Van Hove singularities moving through the Fermi level close to 72 and 86 GPa. The eigenvalues show weak dependence on the temperature at which the pairing interaction is evaluated [23].

In order to examine the electron-phonon pairing and the expected critical temperature from a material-specific perspective, we first determine the strength of the electron-phonon
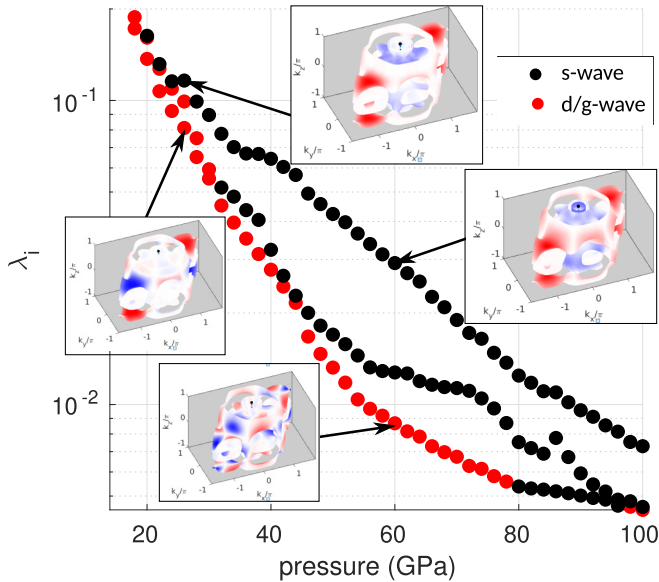

FIG. 3. Spin-fluctuation pairing. Eigenvalues λ_i of the leading and subleading instabilities as a function of pressure as calculated with $U = 0.124$ eV where the critical pressure is $p_c = 16$ GPa. All calculations are at fixed temperature $T = 0.02$ eV. Insets: Gap function $g_i(\mathbf{k})$ on the Fermi surface of the leading s-wave (black circles) state and d/g-wave (red circles) state for two representative pressures of 26 and 60 GPa as indicated by the arrows. Red and blue regions represent two opposite signs of the gap function.
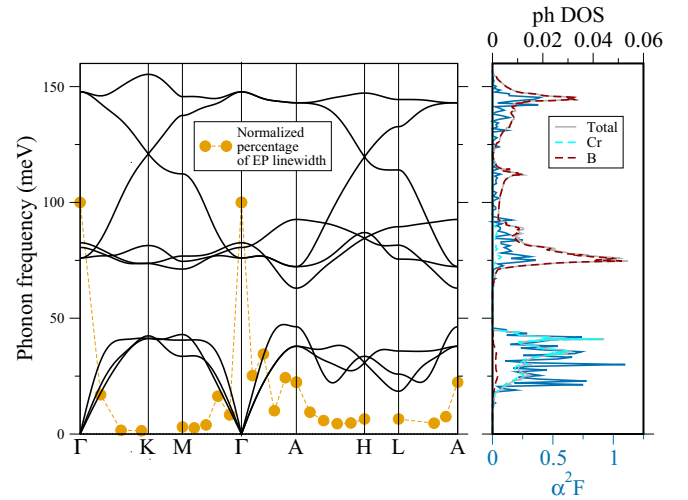

FIG. 4. Phonon dispersion, electron-phonon (EP) linewidth, spectral function [$\alpha^2 F(\omega)$], and phonon density of states (ph DOS) of the relaxed structure at 100 GPa. Normalized percentage of EP linewidth (orange) is equal to $\gamma/\gamma_{\max} \times 100\%$ and is strongly peaked at zone center, Γ.

coupling constant, λ. Experimentally, the system is reported to have the largest T_c around 100 GPa; therefore, we first focus on this pressure region. The relaxed structure at 100 GPa has a ratio $c/a = 0.93$ [whereas $(c/a)_{\exp} = 0.96$] with all phonon modes being stable. We therefore have chosen this structure for establishing convergence criteria for λ with respect to $\mathbf{k}$ mesh, $\mathbf{q}$ mesh, and Gaussian broadening (see Ref. [23]). The converged value of $\lambda = 0.78$ has significant contributions to the electron-phonon spectral function, $\alpha^2 F(\omega)$, from the low-frequency vibrations involving Cr atoms as seen in Fig. 4. Note that the phonon dispersions calculated with the experimental structure [16] exhibit an imaginary acoustic mode along the $\mathbf{k}$ path perpendicular to the honeycomb boron plane. Though this indicates an instability toward a charge density wave state, zero-point vibrational effects can stabilize the conventional structure [23]. Nonetheless, an estimate of the lower bound for $\lambda = 0.60$ could be obtained by excluding the imaginary acoustic mode at 100 GPa.

The electron-phonon linewidth, γ (plotted as $\gamma/\gamma_{\max} \times 100\%$), exhibits maximum contribution around the Brillouin-zone center, i.e., $\mathbf{q} = 0$, which suggests significantly stronger intraband electron-phonon coupling compared to interband contribution, giving rise to conventional s_{++} pairing. With the average phonon frequency softening at lower pressures, T_c is also reduced as pressure goes down. Our computed values of T_c, 14.3 K at 100 GPa and 13.6 K at 60.7 GPa, support this interpretation and justifies our sketch of the electron-phonon driven contribution to T_c in Fig. 1.

Discussions. We have so far investigated the two pairing mechanisms individually, finding that the attractive electron-phonon pairing interaction is dominated by contributions close to $\mathbf{q} = 0$, thus exhibiting a large and positive intraband attractive interaction $V_{\text{intra}}^{\text{EPC}} > 0$, while the interband interaction is much smaller, $V_{\text{inter}}^{\text{EPC}} \ll V_{\text{intra}}^{\text{EPC}}$, leading to critical temperatures of $T_c = 7$ K. The pairing interaction from SF is generically repulsive (negative), but more repulsive for large

momentum transfer so that the interband pairing $V_{\text{inter}}^{\text{SF}} < 0$ is dominating over the intraband pairing $|V_{\text{inter}}^{\text{SF}}| \gg |V_{\text{intra}}^{\text{SF}}|$.

Close to the spin-density-wave instability, the spin fluctuations are enhanced, leading to a sizable pairing interaction, which then quickly decreases with pressure beyond the critical pressure p_c (pressure at which spin fluctuations diverge). Assuming the usual RPA mechanism, one can trace this back to the increase of the electronic bandwidth as a function of pressure, $W(p) \approx W_{\text{AFM}}[1 + x(p - p_c)]$, where W_{AFM} is the bandwidth at the critical pressure p_c and the dependence is assumed to be expanded to first order close to p_c. Taking this into account, we obtain $V_{\text{intra/inter}}^{\text{SF}} \propto [\alpha_{\text{intra/inter}} + x(p - p_c)]^{-1}$, where $\alpha_{\text{intra/inter}}$ describes the closeness of the intra- (inter-) band scattering vectors to a nesting vector giving rise to a peak in the susceptibility [23].

Adding up the electron-phonon and the spin-fluctuation pairing interactions, one then arrives at the qualitative behavior of the critical temperature depicted in Fig. 1, where the spin fluctuations dominate close to p_c and a sign-changing order parameter emerges as the dominant instability. At larger pressures, the critical temperature is expected to decrease until the s_{+-} and s_{++} instabilities have comparable eigenvalues and the critical temperature increases again, since now the pair-breaking contribution from the spin fluctuations $V_{\text{intra}}^{\text{SF}}$ decreases as well and the sum $V_{\text{intra}}^{\text{EPC}} + V_{\text{intra}}^{\text{SF}}$ is dominated by the electron-phonon contribution. Note that despite the small eigenvalues for the SF pairing instability, the electronic contribution to pairing remains finite due to the momentum-independent Hubbard-Hund interaction, and pair breaking will remain non-negligible even at large pressures, where the expected T_c for the "SF alone" pairing is exponentially small. Effective T_c (green line in Fig. 1) thus gets reduced from the T_c computed from EPC only (black line).

Even though isostructural, CrB_2 therefore differs from the prototypical electron-phonon superconductor MgB_2, due to the following aspects: First, due to the presence of Cr $3d$ states, additional effects from these correlated states contribute to the fermiology of the system whereas Mg states in MgB_2 do not take part in the formation of Cooper pairs. Second, the isotropic electron-phonon coupling constants are comparable ($\lambda|_{CrB_2(100 \text{ GPa})} = 0.78$ and $\lambda|_{MgB_2(P=0 \text{ GPa})} = 0.71$); nonetheless, unlike MgB_2, the low-frequency Cr-phonon modes have significant contributions to the EP-spectral function.

Conclusions. In summary, we have presented a hybrid perspective of electron-phonon and spin-fluctuation pairing in order to explain the overall phase diagram of CrB_2 where T_c is found to increase at pressures far away from the antiferromagnetic instability, a behavior not expected for superconductors driven by spin fluctuations alone. Instead, the cooperative and anticooperative effects of the two pairing mechanisms allowed by the presence of a leading instability of the same symmetry explains the larger critical temperature at high pressure (far away from the antiferromagnetic order). Furthermore, the pairing state, while lowering pressure, is predicted to have a crossover from s_{++} to s_{+-} on approaching the quantum critical point with a nonmonotonous behavior of T_c. We have discussed in detail the differences between the well studied MgB_2 and the CrB_2 system; the latter has correlated d states close to the Fermi level and a dominating electron-phonon interaction at small momentum transfer; both of them are required ingredients for the appearance of the hybrid s-wave superconductivity which is expected to exhibit an anisotropic order parameter due to unconventional pairing. An experimental confirmation of the feasibility of this proposal would be a detailed spectroscopic investigation of spin fluctuations and their extension away from the critical point; the available resistivity data [16] so far reveals the antiferromagnetic dome but is unable to pinpoint the presence of fluctuations at higher pressures. Experimental signatures of the proposed scenario would be the nonmonotonous behavior of T_c close to the quantum critical point and the crossover to non-sign-changing order parameter with increasing pressure. The latter could be tested experimentally by observing the effect of disorder. At lower pressures the potential scatterers should lead to a strong suppression of T_c, while the s_{++} state at higher pressures should be almost unaffected according to Anderson's theorem. In fact, the resistivity measurement in Ref. [16] seems to indicate a Fermi-liquid to non-Fermi-liquid crossover at low temperature. The ability to not only tune T_c [27], but also the nature of the superconducting order parameter may open new perspectives in the study of unconventional superconductivity.

[1] J. Bardeen, L. N. Cooper, and J. R. Schrieffer, Theory of superconductivity, Phys. Rev. **108**, 1175 (1957).

[2] G. M. Eliashberg, Zh. Eksp. Teor. Fiz. **38**, 966 (1960) [Sov. Phys. JETP **11**, 696 (1960)].

[3] Y. Nambu, Quasi-particles and gauge invariance in the theory of superconductivity, Phys. Rev. **117**, 648 (1960).

[4] P. Morel and P. W. Anderson, Calculation of the superconducting state parameters with retarded electron-phonon interaction, Phys. Rev. **125**, 1263 (1962).

[5] W. Kohn and J. M. Luttinger, New Mechanism for Superconductivity, Phys. Rev. Lett. **15**, 524 (1965).

[6] C. Gros, R. Joynt, and T. Rice, Superconducting instability in the large-U limit of the two-dimensional Hubbard model, Z. Phys. B **68**, 425 (1987).

[7] S. R. White, D. J. Scalapino, R. L. Sugar, N. E. Bickers, and R. T. Scalettar, Attractive and repulsive pairing interaction vertices for the two-dimensional Hubbard model, Phys. Rev. B **39**, 839 (1989).

[8] I. I. Mazin, D. J. Singh, M. D. Johannes, and M. H. Du, Unconventional Superconductivity with a Sign Reversal in the Order Parameter of LaFeAsO$_{1-x}$F$_x$, Phys. Rev. Lett. **101**, 057003 (2008).

[9] P. Hirschfeld, M. Korshunov, and I. Mazin, Gap symmetry and structure of Fe-based superconductors, Rep. Prog. Phys. **74**, 124508 (2011).

[10] L. Boeri, O. V. Dolgov, and A. A. Golubov, Is LaFeAsO$_{1-x}$F$_x$ an Electron-Phonon Superconductor? Phys. Rev. Lett. **101**, 026403 (2008).

[11] T. S. Nunner, J. Schmalian, and K. H. Bennemann, Influence of electron-phonon interaction on spin-fluctuation-induced superconductivity, Phys. Rev. B **59**, 8859 (1999).

[12] L. Ortenzi, S. Biermann, O. K. Andersen, I. I. Mazin, and L. Boeri, Competition between electron-phonon coupling and spin fluctuations in superconducting hole-doped CuBiSO, Phys. Rev. B **83**, 100505(R) (2011).

[13] O. V. Dolgov, I. I. Mazin, A. A. Golubov, S. Y. Savrasov, and E. G. Maksimov, Critical Temperature and Enhanced Isotope Effect in the Presence of Paramagnons in Phonon-Mediated Superconductors, Phys. Rev. Lett. **95**, 257003 (2005).

[14] N. Witt, J. M. Pizarro, J. Berges, T. Nomoto, R. Arita, and T. O. Wehling, Doping fingerprints of spin and lattice fluctuations in moiré superlattice systems, Phys. Rev. B **105**, L241109 (2022).

[15] I. Schnell, I. I. Mazin, and A. Y. Liu, Unconventional superconducting pairing symmetry induced by phonons, Phys. Rev. B **74**, 184503 (2006).

[16] C. Pei, P. Yang, C. Gong, Q. Wang, Y. Zhao, L. Gao, K. Chen, Q. Yin, S. Tian, C. Li *et al.*, Pressure-induced superconductivity in itinerant antiferromagnet CrB$_2$, arXiv:2109.15213.

[17] J. Nagamatsu, N. Nakagawa, T. Muranaka, Y. Zenitani, and J. Akimitsu, Superconductivity at 39 K in magnesium diboride, Nature (London) **410**, 63 (2001).

[18] I. Mazin and V. Antropov, Electronic structure, electron-phonon coupling, and multiband effects in MgB$_2$, Phys. C (Amsterdam, Neth.) **385**, 49 (2003).

[19] S. Graser, T. A. Maier, P. J. Hirschfeld, and D. J. Scalapino, Near-degeneracy of several pairing channels in multiorbital models for the Fe pnictides, New J. Phys. **11**, 025016 (2009).

[20] M. Altmeyer, D. Guterding, P. J. Hirschfeld, T. A. Maier, R. Valentí, and D. J. Scalapino, Role of vertex corrections in the matrix formulation of the random phase approximation for the multiorbital Hubbard model, Phys. Rev. B **94**, 214515 (2016).

[21] A. Kreisel, Y. Wang, T. A. Maier, P. J. Hirschfeld, and D. J. Scalapino, Spin fluctuations and superconductivity in K$_x$Fe$_{2-y}$Se$_2$, Phys. Rev. B **88**, 094522 (2013).

[22] M. Dürrnagel, J. Beyer, R. Thomale, and T. Schwemmer, Unconventional superconductivity from weak coupling, Eur. Phys. J. B **95**, 112 (2022).

[23] See Supplemental Material at http://link.aps.org/supplemental/10.1103/PhysRevB.108.L020501 for hybrid *s*-wave superconductivity in CrB$_2$ which gives details of the EPC and SF calculations and contains Refs. [16,19,21,22,24,28–34].

[24] P. Giannozzi, S. Baroni, N. Bonini, M. Calandra, R. Car, C. Cavazzoni, D. Ceresoli, G. L. Chiarotti, M. Cococcioni, and I. Dabo, QUANTUM ESPRESSO: A modular and open-source software project for quantum simulations of materials, J. Phys.: Condens. Matter **21**, 395502 (2009).

[25] J. Kortus, I. I. Mazin, K. D. Belashchenko, V. P. Antropov, and L. L. Boyer, Superconductivity of Metallic Boron in MgB$_2$, Phys. Rev. Lett. **86**, 4656 (2001).

[26] A. Bauer, A. Regnat, C. G. F. Blum, S. Gottlieb-Schönmeyer, B. Pedersen, M. Meven, S. Wurmehl, J. Kuneš, and C. Pfleiderer, Low-temperature properties of single-crystal CrB$_2$, Phys. Rev. B **90**, 064414 (2014).

[27] D. N. Basov and A. V. Chubukov, Manifesto for a higher T_c, Nat. Phys. **7**, 272 (2011).

[28] K. Koepernik and H. Eschrig, Full-potential nonorthogonal local-orbital minimum-basis band-structure scheme, Phys. Rev. B **59**, 1743 (1999).

[29] J. P. Perdew and Y. Wang, Accurate and simple analytic representation of the electron-gas correlation energy, Phys. Rev. B **45**, 13244 (1992).

[30] G. Kresse and J. Hafner, *Ab initio* molecular dynamics for liquid metals, Phys. Rev. B **47**, 558 (1993).

[31] S. Baroni, S. de Gironcoli, A. Dal Corso, and P. Giannozzi, Phonons and related crystal properties from density-functional perturbation theory, Rev. Mod. Phys. **73**, 515 (2001).

[32] W. L. McMillan, Transition temperature of strong-coupled superconductors, Phys. Rev. **167**, 331 (1968).

[33] P. B. Allen and R. C. Dynes, Transition temperature of strong-coupled superconductors reanalyzed, Phys. Rev. B **12**, 905 (1975).

[34] J. Beyer, J. B. Hauck, and L. Klebl, Reference results for the momentum space functional renormalization group, Eur. Phys. J. B **95**, 65 (2022).